



· 论 著 ·

探究双层光谱探测器CT在鉴别可切除胰腺导管腺癌与肿块型慢性胰腺炎方面的价值

刘 伟¹, 解添淞¹, 陈 雷², 张泽华², 周正荣^{1, 2}

1. 复旦大学附属肿瘤医院放射诊断科, 复旦大学上海医学院肿瘤学系, 上海 200032;

2. 复旦大学附属肿瘤医院闵行分院放射诊断科, 上海 201100;

[摘要] 背景与目的: 胰腺导管腺癌 (pancreatic ductal adenocarcinoma, PDAC) 与肿块型慢性胰腺炎 (mass-forming chronic pancreatitis, MFCP) 的准确鉴别具有较大的临床意义。双层光谱探测器计算机体层成像 (dual-layer spectral detector computed tomography, DLCT) 在胰腺方面的应用已有一定的探索。本研究旨在探究DLCT在鉴别可切除PDAC与MFCP方面的价值。方法: 回顾性分析2021年9月1日—2023年5月31日复旦大学附属肿瘤医院收治的33例可切除PDAC和19例MFCP患者的临床影像学资料, 术前行DLCT增强扫描, 扫描期相包括动脉期 (arterial phase, AP)、实质期 (parenchymal phase, PP) 和静脉期 (venous phase, VP)。计算DLCT定量指标, 包括衰减变化分数 (attenuation enhancement fraction, AEF)、病灶胰腺实质比 (lesion to parenchyma ratio, LPR)、碘强化分数 (iodine enhancement fraction, IEF)。采用独立样本 t 检验或 χ^2 检验进行统计学分析, 采用二元逻辑回归进行单因素及多因素分析, 采用受试者工作特征 (receiver operator characteristic, ROC) 曲线进行效能评价。 $P < 0.05$ 为差异有统计学意义。结果: 在PDAC与MFCP之间, AEF_{AP/PP}、LPR_{40_VP}、IEF_{PP/VP}、糖类抗原19-9 (carbohydrate antigen 19-9, CA19-9) 及双管征的差异有统计学意义 ($P < 0.05$)。LPR_{40_VP}与IEF_{PP/VP}构成的融合模型具有最佳的鉴别效能, 优于CA19-9、双管征及AEF_{AP/PP} ($P < 0.05$), 其曲线下面积 (area under curve, AUC) 为0.841, 灵敏度为90%, 特异度为73%, 准确度为79%。结论: DLCT在鉴别可切除PDAC与MFCP方面具有一定潜能, 光谱定量参数可以弥补CA19-9、常规CT在鉴别可切除PDAC与MFCP方面的不足。

[关键词] 胰腺导管腺癌; 肿块型慢性胰腺炎; 双层光谱探测器计算机体层成像; 常规计算机体层成像

中图分类号: R735.9 文献标志码: A DOI: 10.19401/j.cnki.1007-3639.2024.01.003

Investigating the value of dual-layer spectral detector CT in distinguishing resectable pancreatic ductal adenocarcinoma from mass-forming chronic pancreatitis

LIU Wei¹, XIE Tiansong¹, CHEN Lei², ZHANG Zehua², ZHOU Zhengrong^{1,2} (1. Department of Radiology, Fudan University Shanghai Cancer Center, Department of Oncology, Shanghai Medical College, Fudan University, Shanghai 200032, China; 2. Department of Radiology, Minhang Branch, Fudan University Shanghai Cancer Center, Shanghai 201100, China)

Correspondence to: ZHOU Zhengrong, E-mail: zhouzr-16@163.com.

[Abstract] **Background and Purpose:** Accurate differentiation of pancreatic ductal adenocarcinoma (PDAC) from mass-forming chronic pancreatitis (MFCP) is clinically significant. The application of dual-layer spectral detector CT (DLCT) in pancreas has been explored. This study aimed to investigate the value of DLCT in distinguishing resectable PDAC from MFCP. **Methods:** We retrospectively collected data of 33 patients with resectable PDAC and 19 patients with MFCP admitted to Fudan University Shanghai Cancer Center from September 1, 2021 to May 31, 2023. Prior to surgery, patients underwent enhanced DLCT scans, including arterial phase (AP), parenchymal phase (PP) and venous phase (VP). DLCT quantitative parameters, including attenuation enhancement fraction (AEF), lesion-to-pancreas ratio (LPR) and iodine enhancement fraction (IEF) were calculated. Difference analysis was conducted using independent sample t -test or

基金项目: 上海市“科技创新行动计划”港澳台科技合作项目 (22490760800); 上海市闵行区医学特色专科建设项目 (2020MWFC05)。

第一作者: 刘伟 (ORCID: 0000-0003-3789-8953), 博士在读, 主治医师。

通信作者: 周正荣 (ORCID: 0000-0002-9922-1000), 博士, 主任医师, 复旦大学附属肿瘤医院闵行分院执行院长, E-mail: zhouzr-16@163.com。

chi-square test. Univariate and multivariate analyses were performed using binary logistic regression. Receiver operating characteristic (ROC) curves were used for performance evaluation. $P < 0.05$ was considered statistically significant. **Results:** Statistically significant differences were observed between PDAC and MFCP in AEF_AP/PP, LPR₄₀_VP, IEF_PP/VP, carbohydrate antigen 19-9 (CA19-9) and double-duct sign (all $P < 0.05$). The spectral combined model composed of LPR₄₀_VP and IEF_PP/VP exhibited the best discriminatory efficacy, surpassing CA19-9, double-duct sign and AEF_AP/PP (all $P < 0.05$). The combined model demonstrated an area under curve (AUC) of 0.841, sensitivity of 90%, specificity of 73%, and accuracy of 79%. **Conclusion:** DLCT has certain potential in differentiating resectable PDAC from MFCP. Spectral quantitative parameters can complement CA19-9 and outcome shortcomings of conventional CT in distinguishing resectable PDAC from MFCP.

[**Key words**] Pancreatic ductal adenocarcinoma; Mass-forming chronic pancreatitis; Dual-layer spectral detector computed tomography; Conventional computed tomography

慢性胰腺炎 (chronic pancreatitis, CP) 是一种长期持续的胰腺炎性病变, 组织学特点为胰腺不可逆损伤所致的胰腺实质的纤维化、萎缩及胰管结构改变^[1-2]。计算机体层成像 (computed tomography, CT) 是CP首选的影像学检查方法, 总体诊断灵敏度为75%^[2], 准确度为77%^[3]。27%~50%的CP在形态学上可呈局灶样或肿块样表现, 形成肿块型CP (mass-forming CP, MFCP)^[4-5]。MFCP在CT上与胰腺导管腺癌 (pancreatic ductal adenocarcinoma, PDAC) 相似, 表现为乏血供肿块^[6], 且两者在实验室检查指标、危险因素及临床表现等方面具有较大的重叠区^[7], 这是造成MFCP误诊为PDAC的主要原因。

目前, MFCP仍以保守治疗为主^[2, 5, 8], 而手术仍是治愈PDAC的唯一手段^[9], 因此区分MFCP与PDAC具有较大的临床意义。虽然灌注CT、磁共振成像 (magnetic resonance imaging, MRI) 可改善鉴别MFCP与PDAC的准确率, 但总体失败率仍不容忽视^[10-12]。经皮活检、超声内镜下引导的细针抽吸活检可以提高准确率, 但容易引起出血、胰漏等并发症^[13-15], 且对于合并CP的肿块, 超声内镜检出PDAC的灵敏度明显降低 (54%)^[15]。CP是PDAC的高危因素之一^[5], 影像学这种无创性检查更适合对其进行监测, 可及时发现恶变征兆。

双层光谱探测器CT (dual-layer spectral detector CT, DLCT) 在胰腺方面的应用已有一定的探索, 它可以提高组织对比度, 从而提高PDAC的检出及对动脉受累的评估效能, 还可以

通过评估胰腺实质纤维化来预测术后胰痿的发生^[16-17], 有望提升CT在鉴别MFCP与PDAC方面的能力, 及时提示CP可疑恶性病变区域, 从而提高活检准确率。另外, DLCT在鉴别MFCP与PDAC方面有一定价值^[18], 但该研究并未与常规CT进行比较, 也未对PDAC进行可切除性筛选。本研究拟探究DLCT在可切除PDAC与MFCP鉴别方面的价值, 并与常规CT进行比较。

1 资料和方法

1.1 患者资料

回顾性分析2021年9月1日—2023年5月31日在复旦大学附属肿瘤医院行胰腺病变手术治疗且病理学检查证实为MFCP或PDAC的患者资料。MFCP定义为组织病理学检查证实为CP且形态学呈局灶样或肿块样表现^[5]。纳入标准: ①术前未进行其他辅助治疗; ②术前2周内行IQon光谱CT上行胰腺多期增强检查; ③图像质量良好, 满足分析要求; ④胰腺肿块可切除性分类均为可切除^[9]。排除标准: ①图像质量不佳; ②临床病理学资料不完整。根据上述标准, 最终纳入33例可切除PDAC和19例MFCP患者。该回顾性研究通过复旦大学附属肿瘤医院伦理学委员会审核, 豁免知情同意。

1.2 DLCT扫描方案

所用设备为DLCT (荷兰Philips公司), 管电压为120 kVp, 管电流采用自动毫安秒技术, 范围为200~300 mAs, 矩阵512×512, 扫描期相包括动脉期 (arterial phase, AP)、实质期

(parenchyma phase, PP) 和静脉期 (venous phase, VP)。经肘正中静脉团注对比剂 [碘佛醇, 碘浓度 (iodine concentration, IC) 为 320 mg/mL, 江苏恒瑞医药股份有限公司], 注射速率为 3.5~5.0 mL/s, 当腹主动脉CT值达到 100 HU 时触发 AP 扫描, 20 s 后开始 PP 扫描, 70 s 后开始 VP 扫描。采用迭代重建技术和光谱重建技术分别获取常规 CT 图像及光谱基图像 (spectral base images, SBI)。

1.3 影像学分析

邀请 2 名放射科医师 (分别具有 7 年和 12 年腹部放射学诊断经验) 进行分析。将 SBI 数据导入 IntelliSpace Portal 软件 (荷兰 Philips 公司) 进行分析。在 40 keV 的虚拟单能级图像 (virtual mono-energetic image, VMI) 上对病灶、胰腺、竖脊肌、腹主动脉区绘制感兴趣区 (region of interest, ROI), 同步出现在常规 CT、IC、有效原子序数 (Z-effective atomic number, Zeff) 图上 (图 1、2), 避开血管、胰管、坏死、钙化。测量指标: 常规 CT 及 VMI 上的 CT 值、IC、Zeff、竖脊肌的标准差。计算指标: ① 光谱曲线斜率 $K = (HU_{40\text{ keV}} - HU_{80\text{ keV}}) / (80 - 40)$; ② 碘强化分数 (iodine enhancement fraction, IEF) $_{AP/PP} = IC_{AP} / IC_{PP} \times 100\%$, $_{AP/VP} = IC_{AP} / IC_{VP} \times 100\%$, $_{PP/VP} = IC_{PP} / IC_{VP} \times 100\%$; ③ 衰变强化分数 (attenuation enhancement fraction, AEF) $_{AP/PP} = HU_{AP} / HU_{PP} \times 100\%$, $_{AP/VP} = HU_{AP} / HU_{VP} \times 100\%$, $_{PP/VP} = HU_{PP} / HU_{VP} \times 100\%$; ④ 病灶胰腺实质比 (lesion to parenchyma ratio, LPR) $= HU_{\text{病灶}} / HU_{\text{胰腺}} \times 100\%$; ⑤ 标准化 IC (normalized IC, NIC) $= IC_{\text{病灶}} / IC_{\text{腹主动脉}} \times 100\%$ 。每个定量指标测量 3 次, 取平均值。

基于 Kirkegård 等^[5] 的研究, 2 名医师评估 CT 形态学征象: ① 导管穿透征; ② 侧支胰管扩张征; ③ 胰管胰腺实质比 ≤ 0.34 ; ④ 钙化移位征; ⑤ 双管征; ⑥ 肠系膜上动脉与肠系膜上静脉直径比 > 1 ; ⑦ 血管包裹征或畸形。①②③ 提示为 MFCP, ④⑤⑥⑦ 为 PDAC。

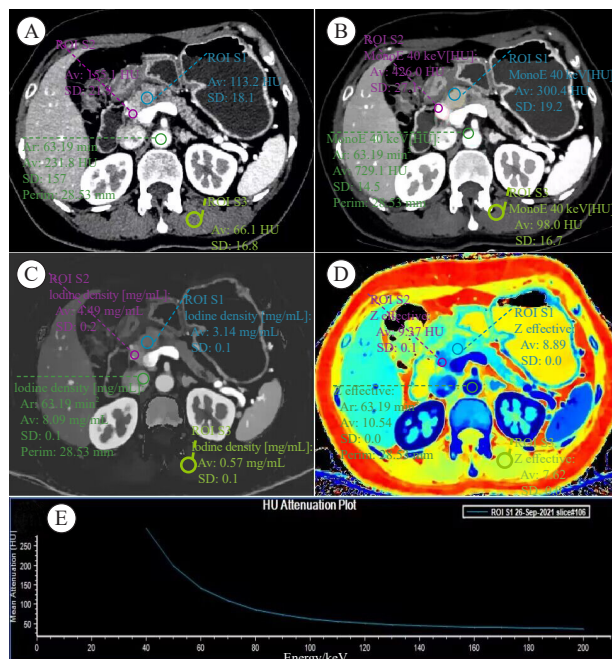


图1 MFCP的CT表现及ROI绘制方法

Fig. 1 The CT performance of MFCP and the method of drawing ROI

A 57-year-old female patient with MFCP. A: Conventional CT image; B: 40 keV virtual mono-energetic image; C: Iodine concentration map; D: Z-effective atomic number map; E: The spectral curve of the MFCP lesion. The yellow circle is located in MFCP, the red circle is located in pancreatic parenchyma, and the green circle is located in abdominal aorta.

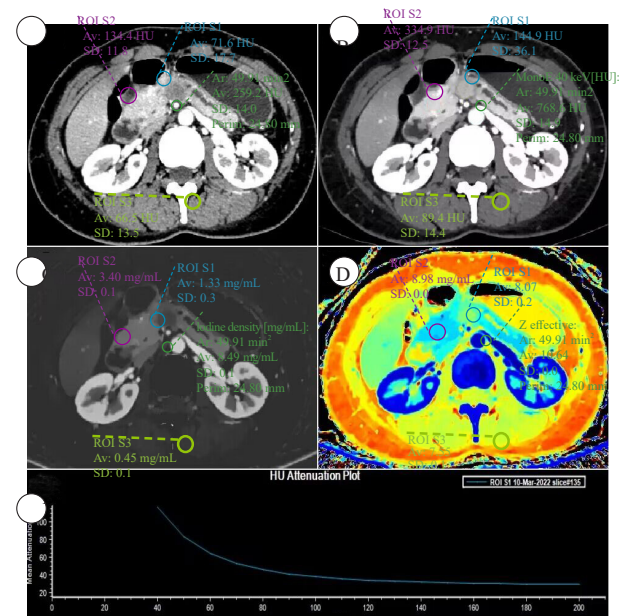


图2 PDAC的CT表现及ROI绘制方法

Fig. 2 The CT performance of PDAC and the method of drawing ROI

A 46-year-old female patient with PDAC. A: Conventional CT image; B: 40 keV virtual mono-energetic image; C: Iodine concentration map; D: Z-effective atomic number map; E: The spectral curve of the PDAC lesion. The yellow circle is located in MFCP, the red circle is located in pancreatic parenchyma, and the green circle is located in abdominal aorta.

1.4 统计学处理

采用SPSS 26软件对数据进行统计学分析。计量资料采用 $\bar{x} \pm s$ 表示,计数资料采用频数表示。采用组内相关系数(interclass correlation coefficient, ICC)及Kappa值进行一致性分析,数值在0.75以上认为一致性较好。采用独立样本 t 检验、 χ^2 检验比较PDAC与MFCP的各个指标之间的差异性。采用向前二元逻辑回归进行单因素及多因素分析。采用方差膨胀因子(variance inflation factor, VIF)对指标进行共线性评价,当 $VIF > 5$ 时,共线问题存在。采用步进回归方法筛选指标,解决共线性问题。最后,采用受试者工作特征(receiver operator characteristic, ROC)曲线评价鉴别效能,并采用DeLong方法进行ROC曲线比较。 $P < 0.05$ 为差异有统计学意义。

2 结果

2.1 患者资料

共纳入52例患者,包括33例可切除PDAC和19例MFCP,其临床和影像学资料的差异性比较见表1。在临床资料中,PDAC出现糖类抗原19-9

(carbohydrate antigen 19-9, CA19-9)异常升高的比例更高。2名医师所评定量指标的ICC范围为0.850(95% CI: 0.708~0.926)~0.942(95% CI: 0.881~0.972),影像学定性资料评价完全一致,表现出良好的一致性。在影像学资料中,PDAC出现双管征的比例更高。

在常规CT定量指标中,PDAC的AEF_AP/PP较MFCP更大(76 ± 13 vs 66 ± 9 , $P = 0.003$)。在PDAC与MFCP之间,光谱定量参数K_AP(1.31 ± 0.60 vs 1.72 ± 0.62 , $P = 0.024$)、K_PP(2.90 ± 1.16 vs 4.13 ± 0.74 , $P < 0.001$)、K_VP(3.06 ± 1.12 vs 4.18 ± 0.82 , $P < 0.001$)、LPR₄₀_PP(62 ± 20 vs 76 ± 14 , $P = 0.003$)、LPR₄₀_VP(86 ± 24 vs 117 ± 24 , $P < 0.001$)、NIC_PP(23 ± 12 vs 30 ± 7 , $P = 0.012$)、Z_{eff}_AP(7.74 ± 0.17 vs 7.86 ± 0.14 , $P = 0.012$)、Z_{eff}_PP(8.22 ± 0.35 vs 8.52 ± 0.24 , $P = 0.002$)和IEF_PP/VP(85 ± 19 vs 106 ± 24 , $P = 0.001$)差异有统计学意义。

2.2 PDAC和MFCP之间光谱定量参数的单因素及多因素分析

单因素分析发现,在光谱定量参数中,LPR₄₀_PP、LPR₄₀_VP和IEF_PP/VP为鉴别PDAC

表1 患者的临床和影像学资料的差异性比较

Tab. 1 The comparison of clinical and imaging data of patients

Data	PDAC (n=33)	MFCP (n=19)	P value
Clinical variables			
Age/year $\bar{x} \pm s$	62.75 ± 10.45	63.95 ± 11.76	0.707*
Gender male/female	16/17	11/8	0.513#
CA19-9 ≤37 U/mL/>37 U/mL	6/27	10/9	0.010#
CA12-5 ≤35 U/mL/>35 U/mL	32/1	19/0	1.000#
CEA ≤5.2 ng/mL/>5.2 ng/mL	30/3	18/1	1.000#
Size/cm $\bar{x} \pm s$	2.50 ± 0.83	2.67 ± 0.66	0.429*
Location head/body and tail	26/7	13/6	0.618#
Imaging morphological variables			
Duct-penetrating sign yes/no	0/33	1/18	0.365#
Collateral duct dilatation yes/no	0/33	0/19	
Duct-to-parenchyma ratio ≤0.34 yes/no	23/10	15/4	0.469#
Displaced calcification yes/no	0/33	0/19	
Double duct sign yes/no	14/19	2/17	0.016#
SMA-to-SMV ratio >1 yes/no	0/33	0/19	
Vessel encasement or deformity yes/no	1/32	0/19	1.000#

*: Independent sample t test; #: χ^2 test. SMA: Superior mesenteric artery; SMV: Superior mesenteric vein.

与MFCP的指标，且无共线性问题。多因素分析发现，LPR₄₀_VP和IEF_PP/VP为鉴别PDAC与MFCP的独立指标，由此建立两者的融合模型（表2）。

2.3 分析各指标在鉴别PDAC与MFCP方面的效能

在鉴别PDAC与MFCP方面，光谱参数LPR₄₀_VP、IEF_PP/VP构建的融合模型的曲线下面积（area under curve, AUC）为0.841（图3，表3），其与双管征（AUC=0.675）、CA19-9（AUC=0.672）、AEF_AP/PP（AUC=0.703）相比表现更优（ $P=0.025$ 、 0.039 、 0.047 ）。另外，LPR₄₀_VP（AUC=0.825）的鉴别效能优于AEF_AP/PP（ $P=0.041$ ）。其中，融合模型具有最高准确度（79%），CA19-9具有最高特异度（82%），AEF_AP/PP具有最高灵敏度（95%）。

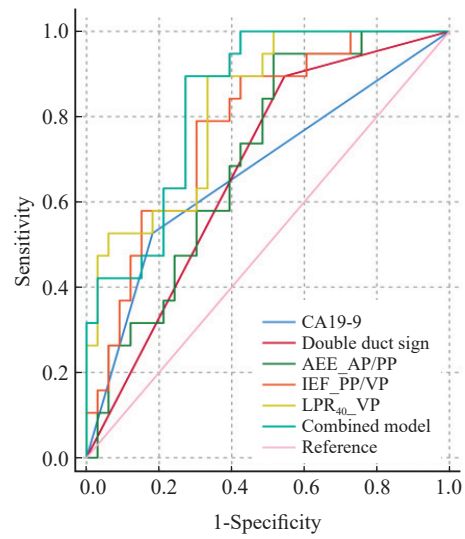


图3 临床及影像指标的ROC曲线分析

Fig. 3 ROC curve analyses of clinical and imaging variables

Double duct sign: Expansion of both common bile duct and main pancreatic duct; AEF: Attenuation enhancement fraction; IEF: Iodine enhancement fraction; LPR₄₀: Lesion to parenchyma ratio on 40 keV virtual mono-energetic images; Combined model: The combination of LPR₄₀_VP and IEF_PP/VP.

表2 光谱定量指标的单因素及多因素分析

Tab. 2 The univariate and multivariate analysis of spectral quantitative variables

Variable	Univariate analysis		VIF	Multivariable analysis	
	OR (95% CI)	P value		OR (95% CI)	P value
LPR ₄₀ _PP/%	1.046 (1.010-1.084)	0.012	3.165		0.111
LPR ₄₀ _VP/%	1.054 (1.022-1.087)	0.001	2.253	1.050 (1.015-1.086)	0.004
IEF_PP/VP/%	1.057 (1.016-1.099)	0.006	1.716	1.051 (1.002-1.102)	0.039

表3 各指标在鉴别PDAC与MFCP方面的效能

Tab. 3 The efficacy of variables in PDAC and MFCP

Variable	AUC (95%CI)	Cutoff value	Sensitivity/%	Specificity/%	Accuracy/%	Youden index
CA19-9	0.672 (0.539-0.806)		53	82	71	0.35
Double duct sign	0.675 (0.563-0.786)		90	46	60	0.36
AEF_AP/PP	0.703 (0.562-0.845)	79%	95	49	65	0.44
LPR ₄₀ _VP	0.825 (0.712-0.937)	91%	90	67	75	0.57
IEF_PP/VP	0.777 (0.648-0.905)	91%	79	70	73	0.49
Combined model	0.841 (0.736-0.945)	0.34	90	73	79	0.63

3 讨 论

MFCP与PDAC的鉴别诊断较为困难。DLCT通过双层探测器分别记录同一球管的高、低能量光子,通过算法迭代重建VMI、IC、Zeff及常规CT图像^[19],可以获取较多的功能参数。光谱定量参数LPR_{40_VP}、IEF_PP/VP在鉴别MFCP与PDAC方面具有一定的价值,这两个参数的融合模型可进一步提高鉴别效能,其AUC为0.841,灵敏度为90%,特异度为73%,准确度为79%。

MFCP灌注CT参数血流量、血容量、血管表面渗透面积均大于PDAC,这与其显微镜下病理学所见相符,MFCP在显微镜下可见微血管密度更高,而纤维化相对较低,故MFCP血流灌注高于PDAC^[10,20]。本研究发现,光谱参数区别这一镜下差异的效能较常规CT参数更高。这是因为常规CT所识别的X线在不同组织中的衰减存在较明显的重叠区,而光谱CT可以将组织内X线的衰减表示为光电效应与康普顿效应的线性组合,可以减小不同物质衰减的重叠区,放大不同组织之间的差异^[21-23],从而更好地区分MFCP与PDAC的血流灌注差异,提高鉴别效能。

基于CT形态学征象区分MFCP与PDAC的AUC为0.84,灵敏度为77%,特异度为86%^[24],Zhang等^[20]通过常规CT征象构建列线图模型,训练集的灵敏度为90%,特异度为75%,验证集的灵敏度为92%,特异度为100%。但本研究中,仅双管征的差异有统计学意义,而特异度明显低于以往研究。这可能是因为本研究所选的病灶较小,且为可切除病变,因此形态学征象不典型。Yin等^[18]采用NIC鉴别MFCP与PDAC的效能较高,AUC>0.95,而本研究虽然NIC_PP表现出差异,但多因素分析发现其并非独立因子。光谱参数LPR_{40_VP}、IEF_PP/VP为区分PDAC与MFCP的独立指标,二者的融合模型可进一步改善鉴别效能,提高特异度,从而弥补双管征的不足。

血清CA19-9在鉴别PDAC与MFCP方面具有一定价值。Su等^[25]研究发现,CA19-9鉴别

PDAC与MFCP的特异度为81%,而灵敏度为81%,明显高于本研究。这与本研究纳入可切除病变及肿瘤专科医院的特点具有一定的关系。一方面,对于可切除PDAC,仅约65%的患者出现CA19-9升高^[26];另一方面,作为肿瘤专科医院,所收治手术的CP呈肿块样表现,且其CA19-9升高比例相对较高,易误诊为PDAC。本研究中,光谱融合模型比CA19-9具有更好的鉴别效能,灵敏度较高,因此可以弥补CA19-9的不足。

本研究存在一定的局限:①本研究为单中心研究,样本量较小,可能存在较大选择偏倚;②因纳入的PDAC为可切除肿块,样本量较少,因此未按照分化程度详细分类;③仅分析PDAC与MFCP,未对胰腺其他乏血供病变进行分析。

综上所述,与常规CT相比,DLCT低能级VMI更有利于胰腺病灶显示。光谱参数能够提高可切除PDAC与MFCP的鉴别效能,可以作为CA19-9、形态学征象及常规CT定量参数的补充指标。

利益冲突声明:所有作者均声明不存在利益冲突。

作者贡献声明:

刘伟:设计研究思路及方案,实施研究过程,收集数据,分析数据,起草论文,修订论文;

解添淞:研究方案可行性调查分析,确定研究对象范围,参与撰写论文,参与论文修订;

陈雷:文献调研与整理;

张泽华:数据测量;

邓薇薇,王誉:提供光谱参数测量及计算方法;

周正荣:提出研究方向,设计论文框架,审核论文,论文最终版本修订。

[参 考 文 献]

- [1] WHITCOMB D C, FRULLONI L, GARG P, et al. Chronic pancreatitis: an international draft consensus proposal for a new mechanistic definition [J]. *Pancreatol*, 2016, 16(2): 218-

- 224.
- [2] SINGH V K, YADAV D, GARG P K. Diagnosis and management of chronic pancreatitis: a review [J] . JAMA, 2019, 322(24): 2422–2434.
- [3] LIAO Q, ZHAO Y P, WU W W, et al. Diagnosis and treatment of chronic pancreatitis [J] . Hepatobiliary Pancreat Dis Int, 2003, 2(3): 445–448.
- [4] KIM T, MURAKAMI T, TAKAMURA M, et al. Pancreatic mass due to chronic pancreatitis: correlation of CT and MR imaging features with pathologic findings [J] . AJR Am J Roentgenol, 2001, 177(2): 367–371.
- [5] KIRKEGÅRD J, MORTENSEN F V, CRONIN-FENTON D. Chronic pancreatitis and pancreatic cancer risk: a systematic review and meta-analysis [J] . Am J Gastroenterol, 2017, 112(9): 1366–1372.
- [6] LUETMER P H, STEPHENS D H, WARD E M. Chronic pancreatitis: reassessment with current CT [J] . Radiology, 1989, 171(2): 353–357.
- [7] WOLSKE K M, PONNATAPURA J, KOLOKYTHAS O, et al. Chronic pancreatitis or pancreatic tumor? A problem-solving approach [J] . Radiographics, 2019, 39(7): 1965–1982.
- [8] GANDHI S, DE LA FUENTE J, MURAD M H, et al. Chronic pancreatitis is a risk factor for pancreatic cancer, and incidence increases with duration of disease: a systematic review and meta-analysis [J] . Clin Transl Gastroenterol, 2022, 13(3): e00463.
- [9] 国家卫生健康委办公厅. 胰腺癌诊疗指南 (2022年版) [J] . 临床肝胆病杂志, 2022, 38(5): 1006–1030.
General Office of National Health Commission. Standard for diagnosis and treatment of pancreatic cancer (2022 edition) [J] . J Clin Hepatol, 2022, 38(5): 1006–1030.
- [10] ASLAN S, NURAL M S, CAMLIDAG I, et al. Efficacy of perfusion CT in differentiating of pancreatic ductal adenocarcinoma from mass-forming chronic pancreatitis and characterization of isoattenuating pancreatic lesions [J] . Abdom Radiol, 2019, 44(2): 593–603.
- [11] SANDRASEGARAN K, NUTAKKI K, TAHIR B, et al. Use of diffusion-weighted MRI to differentiate chronic pancreatitis from pancreatic cancer [J] . AJR Am J Roentgenol, 2013, 201(5): 1002–1008.
- [12] ELSHERIF S B, VIRARKAR M, JAVADI S, et al. Pancreatitis and PDAC: association and differentiation [J] . Abdom Radiol (NY), 2020, 45(5): 1324–1337.
- [13] SEICEAN A, BADEA R, MOLDOVAN-POP A, et al. Harmonic contrast-enhanced endoscopic ultrasonography for the guidance of fine-needle aspiration in solid pancreatic masses [J] . Ultrascall Med, 2017, 38(2): 174–182.
- [14] FACCIORUSSO A, MARTINA M, BUCCINO R V, et al. Diagnostic accuracy of fine-needle aspiration of solid pancreatic lesions guided by endoscopic ultrasound elastography [J] . Ann Gastroenterol, 2018, 31(4): 513–518.
- [15] FRITSCHER-RAVENS A, BRAND L, KNÖFEL W T, et al. Comparison of endoscopic ultrasound-guided fine needle aspiration for focal pancreatic lesions in patients with normal parenchyma and chronic pancreatitis [J] . Am J Gastroenterol, 2002, 97(11): 2768–2775.
- [16] BEER L, TOEPKER M, BA-SSALAMAH A, et al. Objective and subjective comparison of virtual monoenergetic vs polychromatic images in patients with pancreatic ductal adenocarcinoma [J] . Eur Radiol, 2019, 29(7): 3617–3625.
- [17] SHI H Y, LU Z P, LI M N, et al. Dual-energy CT iodine concentration to evaluate postoperative pancreatic fistula after pancreatoduodenectomy [J] . Radiology, 2022, 304(1): 65–72.
- [18] YIN Q H, ZOU X N, ZAI X D, et al. Pancreatic ductal adenocarcinoma and chronic mass-forming pancreatitis: differentiation with dual-energy MDCT in spectral imaging mode [J] . Eur J Radiol, 2015, 84(12): 2470–2476.
- [19] GROÙE HOKAMP N, MAINTZ D, SHAPIRA N, et al. Technical background of a novel detector-based approach to dual-energy computed tomography [J] . Diagn Interv Radiol, 2020, 26(1): 68–71.
- [20] ZHANG H, MENG Y H, LI Q, et al. Two nomograms for differentiating mass-forming chronic pancreatitis from pancreatic ductal adenocarcinoma in patients with chronic pancreatitis [J] . Eur Radiol, 2022, 32(9): 6336–6347.
- [21] YEH B M, SHEPHERD J A, WANG Z J, et al. Dual-energy and low-kVp CT in the abdomen [J] . AJR Am J Roentgenol, 2009, 193(1): 47–54.
- [22] GHASEMI SHAYAN R, OLADGHAFFARI M, SAJJADIAN F, et al. Image quality and dose comparison of single-energy CT (SECT) and dual-energy CT (DECT) [J] . Radiol Res Pract, 2020, 2020: 1403957.
- [23] SAKABE D, FUNAMA Y, TAGUCHI K, et al. Image quality characteristics for virtual monoenergetic images using dual-layer spectral detector CT: comparison with conventional tube-voltage images [J] . Phys Med, 2018, 49: 5–10.
- [24] REN S, ZHANG J J, CHEN J Y, et al. Evaluation of texture analysis for the differential diagnosis of mass-forming pancreatitis from pancreatic ductal adenocarcinoma on contrast-enhanced CT images [J] . Front Oncol, 2019, 9: 1171.
- [25] SU S B, QIN S Y, CHEN W, et al. Carbohydrate antigen 19-9 for differential diagnosis of pancreatic carcinoma and chronic pancreatitis [J] . World J Gastroenterol, 2015, 21(14): 4323–4333.
- [26] SINGH S, TANG S J, SREENARASIMHAIAH J, et al. The clinical utility and limitations of serum carbohydrate antigen (CA19-9) as a diagnostic tool for pancreatic cancer and cholangiocarcinoma [J] . Dig Dis Sci, 2011, 56(8): 2491–2496.

(收稿日期: 2023-08-28 修回日期: 2023-12-15)